Dynamics of Light and Nitrogen Distribution during Grain Filling within Wheat Canopy[1][OA]

Jessica Bertheloot, Pierre Martre*, and Bruno Andrieu

INRA, UMR 1091 Environnement et Grandes Cultures, F–78 850 Thiverval-Grignon, France (J.B., B.A.); AgroParisTech, UMR 1091 Environnement et Grandes Cultures, F–78 850 Thiverval-Grignon, France (J.B., B.A.); INRA, UMR 1095 Génétique, Diversité et Ecophysiologie des Céréales, F–63 100 Clermont-Ferrand, France (P.M.); and Université Blaise Pascal, UMR 1095 Génétique, Diversité et Ecophysiologie des Céréales, F–63 100 Clermont-Ferrand, France (P.M.)

In monocarpic species, during the reproductive stage the growing grains represent a strong sink for nitrogen (N) and trigger N remobilization from the vegetative organs, which decreases canopy photosynthesis and accelerates leaf senescence. The spatiotemporal distribution of N in a reproductive canopy has not been described in detail. Here, we investigated the role of the local light environment on the spatiotemporal distribution of leaf lamina N mass per unit leaf area (SLN) during grain filling of field-grown wheat (*Triticum aestivum*). In addition, in order to provide some insight into the coordination of N depletion between the different vegetative organs, N dynamics were studied for individual leaf laminae, leaf sheaths, internodes, and chaff of the top fertile culms. At the canopy scale, SLN distribution paralleled the light gradient below the flag leaf collar until almost the end of grain filling. On the contrary, the significant light gradient along the flag leaf lamina was not associated with a SLN gradient. Within the top fertile culms, the time course of total (alive + necrotic tissues) N concentration of the different laminae and sheaths displayed a similar pattern. Another common pattern was observed for internodes and chaff. During the period of no root N uptake, N depletion of individual laminae and sheaths followed a first-order kinetics independent of leaf age, genotype, or N nutrition. The results presented here show that during grain filling, N dynamics are integrated at the culm scale and strongly depend on the local light conditions determined by the canopy structure.

Nitrogen (N) plays a key role in crop productivity. Indeed, N is involved in the functioning of meristematic tissues, in photosynthesis, and in the determination of the protein content of harvested organs. Up to 75% of the reduced N in cereal leaves is located in the mesophyll cells, mainly as Rubisco, and is involved in photosynthetic processes (for a detailed discussion, see Evans, 1989). During the reproductive stage, N is translocated to growing grains, which decreases the photosynthetic capacity and indirectly hampers the ability of roots to further take up N. Finally, this results in the death of vegetative organs. The involvement of N in both biomass accumulation and grain protein concentration determination results in complex interactions between carbon and N metabolisms that determine crop productivity and quality (Triboi and Triboi-Blondel, 2002).

In wheat (*Triticum aestivum*), modern cultivars appear to be close to the maximum theoretical harvest index (shoot to grain biomass ratio; Austin, 1999); over the last decade, genetic gains in productivity have been mostly achieved through the increase of total aboveground biomass (Shearman et al., 2005). This contrasts with previous gains, which were achieved mostly by increased allocation of biomass to grains. Two possibilities related to the improvement of N distribution among plant organs have been suggested to increase crop productivity (Dreccer et al., 1998). The first one is to select cultivars with a greater capacity to store N in nonphotosynthetic organs, such as internodes: that allows the translocation of a larger amount of N to grains without reducing plant photosynthetic capacity (Martre et al., 2007). This is one trait associated with the ''stay-green'' behavior resulting in delayed leaf senescence and improved grain yield (Borrell et al., 2001). The second possibility is to improve the vertical distribution of N among leaves. Theoretical studies have suggested that canopy photosynthesis would be maximized if N is preferentially allocated to the more illuminated leaves (Field, 1983). A vertical N distribution that follows the light gradient would allow higher photosynthesis compared with that expected from a uniform N distribution (Mooney and Gulmon, 1979). The role of N dynamics on canopy photosynthesis and crop productivity will likely become even more important in the future because of the increase of atmospheric CO_2 concentration (Kim et al., 2001; Anten et al., 2004).

N distribution among leaf laminae has often been analyzed through the ''optimization'' theory (Hirose

[1] This work was supported by the Agence Nationale de la Recherche Génoplante Initiative (grant no. ANR–06–GPLA–016–003).

* Corresponding author; e-mail pmartre@clermont.inra.fr.

The author responsible for distribution of materials integral to the findings presented in this article in accordance with the policy described in the Instructions for Authors (www.plantphysiol.org) is: Pierre Martre (pmartre@clermont.inra.fr).

[OA] Open Access articles can be viewed online without a subscription.

www.plantphysiol.org/cgi/doi/10.1104/pp.108.124156

and Werger, 1987). This theory suggests that lamina N distribution within a vegetative canopy optimizes whole canopy photosynthesis. It implies that, within a dense canopy, leaf lamina N distribution is driven by the light gradient such that leaf lamina N mass per unit leaf area (SLN) follows an exponential function of the downward cumulative leaf area index with an extinction coefficient for N (K_N) equal to that for light (K_L). Nevertheless, until now, an understanding of N distribution within vegetative canopies has not been provided by the optimization theory (Kull, 2002). Observed N gradients are generally less steep than predicted with the optimization theory, and there are numerous cases in which experimental evidence does not back up the hypothesis that SLN follows an exponential gradient (Dreccer et al., 1998). Moreover, there are several limitations in optimization theory calculations (for a detailed discussion, see Reynolds and Chen, 1996). Chen et al. (1993) propose an alternative approach, the coordination theory, which explicitly takes photosynthetic processes into account at the leaf scale to explain the relationship between light and N vertical distribution in vegetative canopies. Here, SLN is computed to maintain a balance between the Rubisco-limited rate of carboxylation and the electron transport-limited rate of carboxylation, which depends on the amount of intercepted light. However, this approach only describes processes at the individual leaf scale and does not account for the impact of the overall plant N status on the vertical leaf N distribution. For this reason, the application of this coordination theory has been very limited.

Relatively little attention has been paid to the pattern of N distribution among individual organs during the reproductive stage of monocarpic species. Available studies either discuss the applicability of the optimization theory during the reproductive stage, focusing on leaf laminae only (Sadras et al., 1993; Drouet and Bonhomme, 1999), or neglect the role of light, focusing on the filling of reproductive organs (Sadras et al., 2000). For sunflower (*Helianthus annuus*) canopy, important changes in leaf lamina N distribution have been reported during the grain-filling period (Sadras et al., 1993); however, the N profile remained close to the photosynthetic optimum almost until physiological maturity (Connor et al., 1995). These studies focused only on leaf lamina N; however, during the reproductive stage, grains represent a strong sink for N, and vegetative organs other than leaf laminae contribute significantly to grain N and plant N dynamics. For instance, Simpson et al. (1983) reported that for wheat at mid grain filling, leaves (i.e. leaf laminae and sheaths) contribute 40%, glumes 23%, stems 23%, and roots 16% of the daily rate of grain N accumulation.

The aim of this study was to analyze N distribution within the wheat canopy during the reproductive stage, taking into account the effect of both the local light environment and N translocation to grains. We asked the following set of questions. Is the vertical leaf N distribution related to light distribution during the grain-filling period? Does the time course of N mass per unit dry mass during grain filling follow a similar pattern in all vegetative organs? More specifically, does N depletion in the different vegetative organs follow unique first-order kinetics in the period of no apparent root N uptake? To investigate these questions, we studied in the field two bread wheat cultivars, Apache and Isengrain, from anthesis to grain maturity. To take into account local light environment and N translocation from individual organs to grains, N dynamics were characterized for both vertical canopy layers and individual organs. We explicitly took into account the different vegetative organs (i.e. leaf laminae, leaf sheaths, internodes, and chaff). This study provides new insights into the mechanisms and driving variables governing N dynamics during the reproductive stage for wheat, both at the organ and whole plant levels. They provide the basis to construct a functional model at the whole plant level as well as for the integration of results at the molecular level into the context of whole plant physiology. Such an integrated knowledge would greatly enhance our chances of achieving genetic improvement in yield and crop N use efficiency.

RESULTS

Apache and Isengrain Had Different Patterns of Apparent Root N Uptake and N Translocation during the Grain-Filling Period

At anthesis, the two cultivars had similar green area index (GAI; surface area of all green tissues per unit ground area; $P = 0.67$) and leaf area index (LAI; surface area of leaf laminae tissues per unit ground area; $P = 0.49$; Fig. 1A), respectively. LAI and GAI decreased slowly until 500°Cd (degree-days) and 600°Cd after anthesis for Apache and Isengrain, respectively. Then, the decrease accelerated. The duration of the grain-filling period was similar for both cultivars: the duration of grain dry mass accumulation was 855 ± 79°Cd and 808 ± 59°Cd for Apache and Isengrain, respectively, while the duration of grain N accumulation was 912 ± 79°Cd and 988 ± 80°Cd for Apache and Isengrain, respectively (Fig. 1B). For Apache, all vegetative tissues were necrotic at the end of the grain N accumulation period, whereas Isengrain retained some green tissues in the stem (including leaf sheaths, internodes, and ear peduncle), which represented a GAI of 0.22.

At anthesis, total canopy N per unit ground area was 19% higher for Isengrain compared with Apache, although not significantly so ($P = 0.061$; Fig. 1B). This difference remained until 400°Cd after anthesis. Leaf laminae, chaff, and stems all contributed to the differences observed (Fig. 1, C and D). At anthesis, on the one hand, total lamina N per unit ground area was 20% higher for Isengrain than for Apache ($P = 0.03$; Fig. 1C), despite the lower LAI. On the other hand, Isengrain chaff contained 43% more N mass per unit

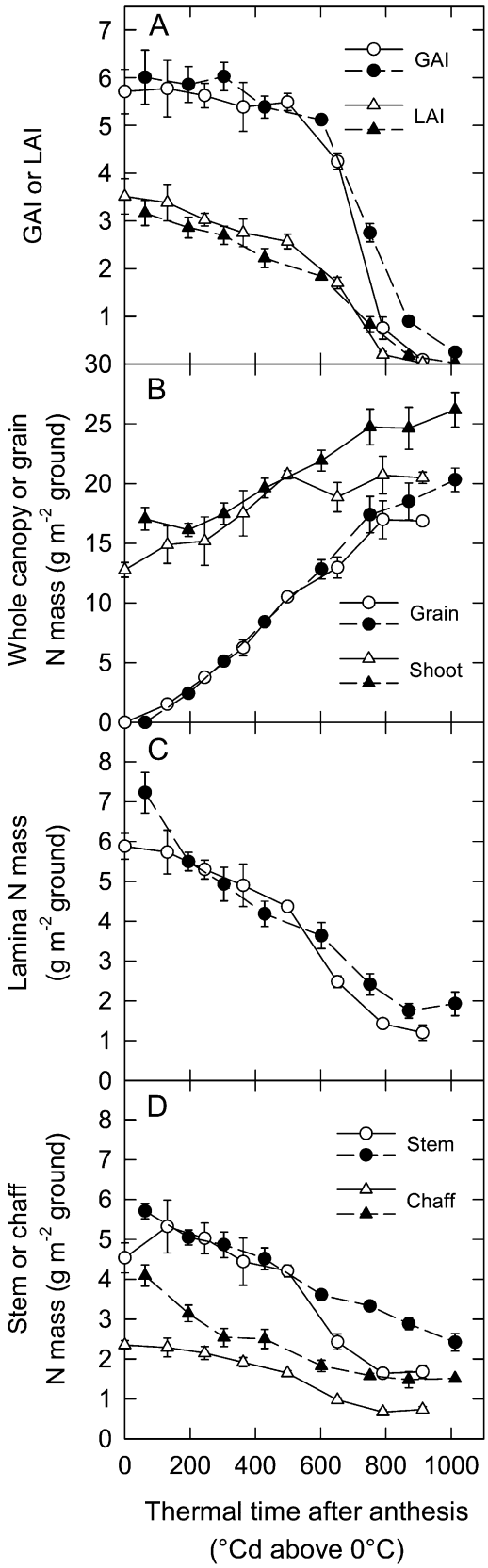

Figure 1. Total and lamina GAI (A), grain and whole canopy N mass per unit ground area (B), lamina N mass per unit ground area (C), and stem (i.e. leaf sheaths and internodes) and chaff N mass per unit ground area (D) versus thermal time after anthesis for crops of the winter bread wheat cultivars Apache (white symbols) and Isengrain (black symbols) grown in the field with nonlimiting N supply. Data are means ± 1 SE for $n = 3$ independent replicates.

ground area than those of Apache ($P < 0.001$; Fig. 1D) because of a 1.5 times higher dry mass per unit ground area (Table I) with similar N mass per unit dry mass (data not shown). Finally, at anthesis, the stem contained more N mass per unit ground area in Isengrain (Fig. 1D), but this was related to a delayed peduncle extension in Apache; the difference no longer existed after 130°Cd, when Apache had completed stem extension, and this held true until 500°Cd.

Vegetative organs lost 74% and 66% of their N mass between anthesis and the end of N grain filling for Apache and Isengrain, respectively (Fig. 1, C and D). On average, for both cultivars, leaf laminae contributed 27% to the N transfer to the grains, stem contributed 18%, and chaff contributed 11%. The remaining fraction came from root N uptake or root N remobilization. As assessed from the increase in whole canopy N mass per unit ground area (Fig. 1B), apparent root N uptake represented 39% and 45% of grain N mass at maturity for Apache and Isengrain, respectively. These two cultivars also differed in the time course of postanthesis apparent root N uptake (Fig. 1B). For Apache, whole canopy N mass per unit ground area increased for 500°Cd after anthesis. After 500°Cd, no significant increase in canopy N mass was observed. The end of canopy N accumulation was concomitant with an increase in the rate of N depletion in all vegetative organs (Fig. 1, C and D). In contrast, for Isengrain, the increase in whole canopy N mass per unit ground area started about 200°Cd after anthesis and took place until 800°Cd. Moreover, the rate of N depletion in the vegetative organs of Isengrain did not show any abrupt change during grain filling.

At maturity, although the differences were not statistically significant at the 5% level, whole canopy and grain N mass per unit ground area were 22% ($P = 0.06$) and 17% ($P = 0.07$) higher for Isengrain than for Apache (Fig. 1B). On the contrary, no difference between the two cultivars in whole canopy and grain dry mass per unit ground area was observed at maturity (Table I).

At anthesis, SLN, averaged over the depth of the canopy, was 17% higher ($P = 0.004$) for Isengrain than for Apache (Fig. 2A). This difference was not due to leaf lamina dry mass per unit leaf area (SLM; $P = 0.15$) but to higher N concentration ($P = 0.004$) in the green tissues of Isengrain compared with those of Apache (Fig. 2, B and C). For both cultivars, after anthesis, most of the variations in SLN were due to variations in N concentration. During the first 400°Cd after anthesis, SLN and N concentration in green lamina tissues decreased faster for Isengrain than for Apache, whereas after 600°Cd, they decreased faster for Apache than for Isengrain.

Table I. *Crop, stem, lamina, sheath, and chaff dry mass (DM) at anthesis, crop DM and grain yield at maturity, and yield components for the wheat cultivars Apache and Isengrain grown in the field with nonlimiting N supply*

Data are means ± 1 SE ($n = 3$ independent replicates). *P*, probability that the cultivars are different following unpaired *t* tests.

Growth Stage	Variable	Cultivar		*P*
		Apache	Isengrain	
Anthesis	Total crop DM (g DM m^{-2} ground)	882 ± 52	1,004 ± 76	0.22
	Stem DM (g DM m^{-2} ground)	517 ± 30	583 ± 45	0.25
	Lamina DM (g DM m^{-2} ground)	208 ± 22	217 ± 44	0.64
	Chaff DM (g DM m^{-2} ground)	132 ± 7	202 ± 14	0.001
Maturity	Total crop DM (g DM m^{-2} ground)	1,851 ± 183	1,909 ± 102	0.79
	Grain yield (g DM m^{-2} ground)	930 ± 86	942 ± 51	0.91
	Grain number (grain m^{-2} ground)	24,169 ± 2,351	26,302 ± 1,499	0.49
	Ear number (ear m^{-2} ground)	548 ± 46	528 ± 40	0.76
	Grain number per ear	44 ± 1	50 ± 1	0.010
	Average grain DM (mg DM $grain^{-1}$)	38.9 ± 0.5	36.0 ± 0.3	0.012

The Distribution of Light with Canopy Depth Did Not Change during the Postanthesis Period

The vertical distribution of photosynthetic photon flux density (PPFD), expressed relative to PPFD above the canopy (I/I_0), was well described by an exponential function of the distance from the top of the canopy (all $r^2 > 0.92$ for the different measurement dates). The exponential coefficient did not change significantly during the reproductive stage, even at crop maturity, when all tissues were dead ($P = 0.48$ and 0.45 for Apache and Isengrain, respectively; Fig. 3, A and B). Thus, tissue death did not significantly modify light attenuation within the canopy. The slight variations were most likely due to differences in cloudiness (ratio of direct to diffuse PPFD) between the successive days of measurements and to the heterogeneity of the canopy, since the successive measurements were done in different parts of the experimental plots.

Consistently, the relationship between I/I_0 and cumulative GAI was constant until 500°Cd and 600°Cd after anthesis for Apache ($P = 0.059$) and Isengrain ($P = 0.096$), respectively (Fig. 3, C and D), which corresponded to the onset of the phase of rapid decrease of GAI (Fig. 1A). During that period, the relationship was exponential and the light extinction coefficient (K_L) was not significantly different ($P = 0.12$) for Apache and Isengrain, averaging 0.42 ± 0.01. During the period of rapid GAI decrease, the proportion of dead tissues increased without change in light distribution with canopy depth. Therefore, the relationship between I/I_0 and cumulative GAI changed markedly.

Below the Level of Flag Leaf Collar, N Vertical Distribution in Green Lamina Tissues Followed the Light Gradient from Anthesis until the Onset of the Rapid GAI Decrease

Light interception and CO_2 assimilation are intrinsically area-based processes; therefore, analysis of leaf N content in relation to light distribution is most meaningful when expressed per unit leaf area. For both cultivars, no SLN gradient was observed in the upper part of the canopy (Fig. 4). Until approximately 350°Cd and 450°Cd after anthesis for Apache and Isengrain, respectively, the height of the flag leaf collar (C1) delimited this upper zone with constant SLN (Fig. 4, A and B). Most of the lower leaf laminae did not pass this level, so that the constant SLN in the upper part of the canopy mainly reflected the absence of a SLN gradient within the flag leaf lamina. Lower in the canopy, SLN decreased with I/I_0 and an almost constant exponential relationship between cumulative GAI and SLN was observed between anthesis and the onset of the rapid GAI decrease (Fig. 4, C and D). This relationship was characterized by the N extinction coefficient K_N. During that period, SLN decreased in the upper part of the canopy despite no significant change for lower leaf lamina tissues. For both cultivars, the vertical gradient of SLN was due to high SLM and N concentration in green lamina tissues above the flag leaf collar, but below the flag leaf collar it was mostly due to variations of N concentration in green tissues (data not shown).

The K_N to K_L ratio was calculated for the canopy layers below the flag leaf collar between anthesis and the end of grain filling. At anthesis, K_N/K_L was not significantly different ($P = 0.30$) for the two cultivars and averaged 0.92 ± 0.05 (Fig. 5). Therefore, the vertical distribution of N at anthesis was close to the optimum, as defined in the optimization theory (Hirose and Werger, 1987). Until almost the end of grain filling, K_N/K_L did not change significantly for both cultivars ($P = 0.15$ and 0.22 for Apache and Isengrain, respectively).

During the Reproductive Stage, the Dynamics of N Concentration Were Similar for All Laminae and Sheaths But Were Unlike the Dynamics in Stem Internodes, Ear Peduncles, and Chaff

The time course of N concentration for each vegetative organ of the top fertile culms is presented for

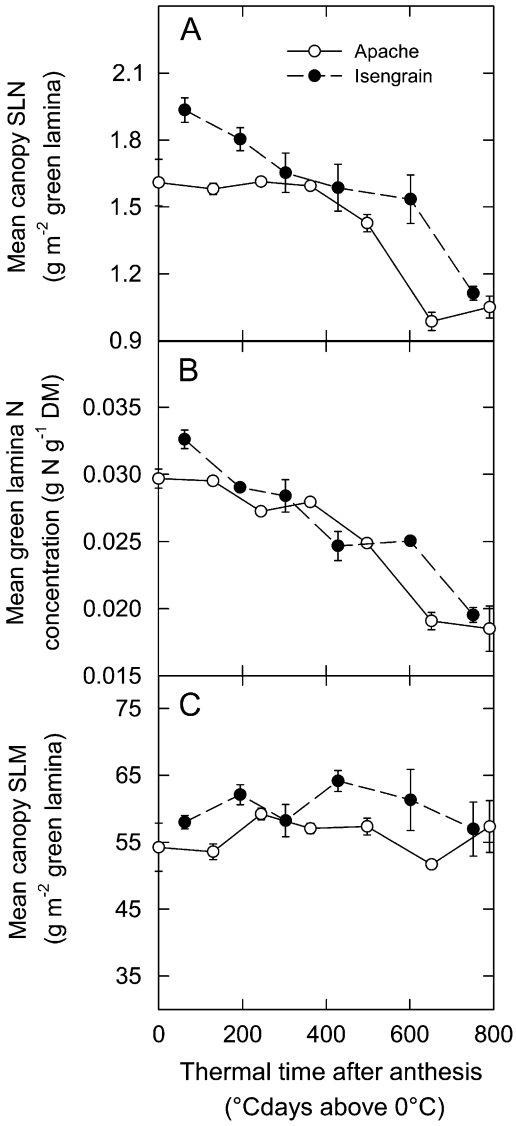

Figure 2. Mean canopy leaf lamina N mass per unit leaf area (A), mean canopy green lamina N concentration (B), and mean canopy leaf lamina dry mass per unit leaf area (C) versus thermal time after anthesis averaged over the depth of the canopy for crops of the winter bread wheat cultivars Apache (white symbols) and Isengrain (black symbols) grown in the field with nonlimiting N supply. Data are means ± 1 SE for $n = 3$ independent replicates. The y axes have been scaled so that a similar percentage of variations in the three panels represents the same fraction of the full scale. DM, Dry mass.

Apache only (Fig. 6). Similar results were observed for Isengrain. At anthesis, within any phytomer, there was a consistent ranking of N concentration, the lamina being richer than the sheath and the sheath being richer than the internode. This ranking persisted until the end of grain filling. Among phytomers, N concentration of laminae, sheaths, and internodes decreased from the top to the bottom of the culms. Although laminae of different ranks had different N concentrations at anthesis, their N concentration decreased to a minimum value of $7.9 \pm 0.7 \times 10^{-3}$ g N g^{-1} dry mass between 800°Cd and 900°Cd after anthesis. N concentration of sheaths, internodes, chaff, and ear peduncle all decreased down to a minimum value of $3.5 \pm 0.9 \times 10^{-3}$ g N g^{-1} dry mass. The remaining N at the end of grain filling was taken to be structural N.

Figure 6 suggests that the relative time course of N concentration was similar for individual laminae and sheaths independent of their age and position in the canopy. Similarly, the time course of N concentration in chaff, individual internodes, and the ear peduncle seems to follow a similar pattern but is different from that of laminae and sheaths. In order to test this hypothesis, the patterns of N concentration were rescaled as described in ''Materials and Methods'' (Eq. 6). To analyze only organs presenting a significant amount of nonstructural N, the upper four laminae, the upper two sheaths, and the internodes, chaff, and ear peduncle were used in this analysis during the period when their N concentration was at least 1.2 times their structural N concentration.

After rescaling, the same pattern described the behavior of all leaf laminae and sheaths, showing that N depletion occurred concomitantly and with the same relative rate in individual leaves of the top fertile culms (Fig. 7). Internodes, chaff, and ear peduncle also followed a similar pattern, but one that was different from that of the leaf laminae and sheaths. During the first half of the reproductive stage, the N concentration of the internodes, chaff, and ear peduncles decreased faster than that for individual laminae and sheaths, whereas the opposite was observed during the second half of the reproductive stage.

A Single First-Order Kinetics Described N Depletion for Laminae Independent of Leaf Age, Genotype, or N Nutrition

It has been shown that the degradation of Rubisco follows first-order kinetics (Irving and Robinson, 2006). Therefore, we tested the hypothesis that first-order kinetics might describe the pattern of N depletion during the period when apparent root N uptake is negligible.

We discarded the measurements corresponding to periods of apparent root N uptake, identified by an increase in whole canopy N, as well as those corresponding to N concentrations lower than 1.2-fold the structural N concentration. As a consequence, we could only use data for Apache laminae, sheaths, and chaff between 500°Cd and 700°Cd after anthesis. To include more data, we used a second data set from an independent field experiment with the winter bread wheat cultivar Thésée involving nine N treatments. The combined data set provided a wide range of crop N status values at anthesis and after anthesis. No postanthesis apparent root N uptake was observed for two treatments of Thésée (M0 and H0); therefore, for these treatments, the analysis covered the whole reproductive period.

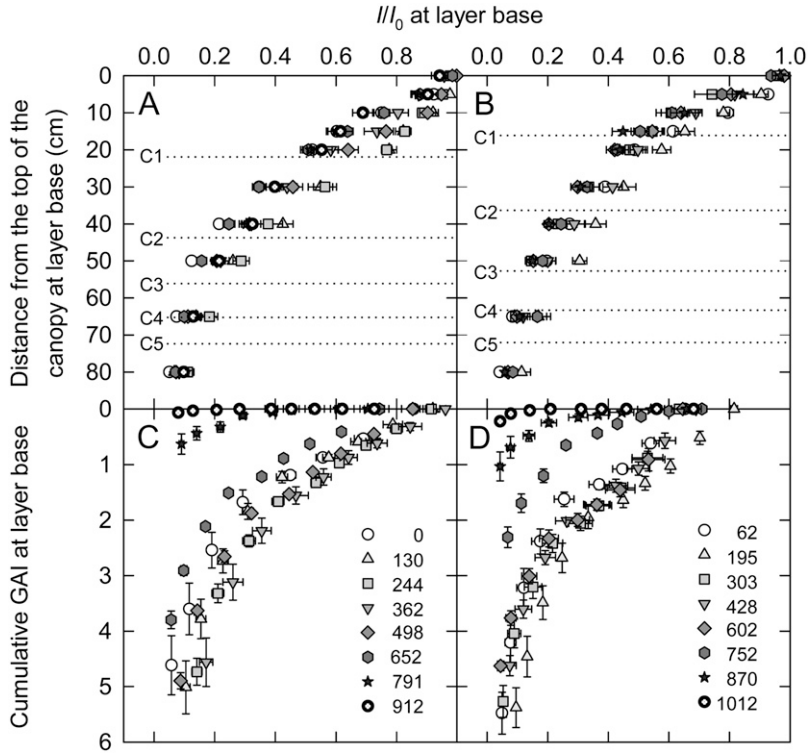

Figure 3. Distance from the top of the canopy (A and B) and cumulative GAI counted from the top of the canopy (C and D) versus relative PPFD determined at different times (expressed as thermal time; base 0°C) between anthesis and maturity for crops of the bread wheat cultivars Apache (A and C) and Isengrain (B and D) grown in the field with nonlimiting N supply. The horizontal dotted lines indicate the height of the collar of the top fertile culm leaves (C1–C5). Data are means ± 1 SE for $n = 3$ independent replicates.

A single value for the relative rate of N depletion (k) was determined for individual culm laminae from the different N treatments for Thésée. A k value of 0.0035 $[°Cd]^{-1}$ was found to minimize the root mean square error (RMSE) between observed and predicted values, and a first-order kinetics with a unique coefficient k could accurately predict N depletion of individual laminae of Thésée grown under contrasted N fertilization treatments ($r^2 = 0.74$, degrees of freedom = 17, $P < 0.001$). Then, we evaluated the ability of the model to predict N depletion between successive sampling dates for each individual organ (experiments 1 and 2) as well as for the whole stem in the case of the second data set (Fig. 8). Simulated and observed values of N depletion for stem, sheath, and chaff were well correlated ($r^2 = 0.79$, degrees of freedom = 19, $P < 0.001$), but N depletion was systematically overestimated by the model, leading to a high relative error of prediction (relative RMSE [RRMSE] = 128% and 251% for stem and chaff of Thésée, and RMSE = 33.8% and 21.4% for chaff and individual sheaths of Apache, respectively). For the individual laminae of Apache and Thésée grown with different rates and timings of N supply, observed N depletions were accurately simulated, with RRMSE of 7% and 14.1%, respectively. Therefore, the rate constant of lamina sheaths and chaff N depletion during grain filling was mostly independent of their age, N status, or genotype, but the rate constant for the laminae was higher than that for the sheaths and chaff.

DISCUSSION

In dense vegetative canopies, light is the main factor controlling leaf N distribution. A linear or power relationship is usually observed between incident PPFD and SLN, which tends to optimize the canopy photosynthesis (Dreccer et al., 2000; Lötscher et al., 2003). How the relationship between PPPD and SLN changes during the productive stage has not been studied in detail for monocotyledons yet. Here in the field, spatiotemporal changes in N distribution were analyzed during the reproductive stage for dense canopies of wheat. Emphasis was on the persistence of the role of the local PPFD environment during that period, at which time a strong sink for N (growing grains) triggers N translocation from the vegetative organs. In addition, in order to provide some insight into the coordination of N depletion between vegetative organs, the dynamics of N concentration was studied for the different organs of the top fertile culms from anthesis to crop maturity. This study provides a comprehensive picture of N dynamics within the canopy at the crop and organ levels during the critical period of grain filling.

The Vertical Leaf N Distribution during the Grain-Filling Period Is Related to Light Distribution, But the Light Signal Appears Integrated at the Leaf Level

The vertical distribution of PPFD throughout the canopy did not significantly change during the reproductive

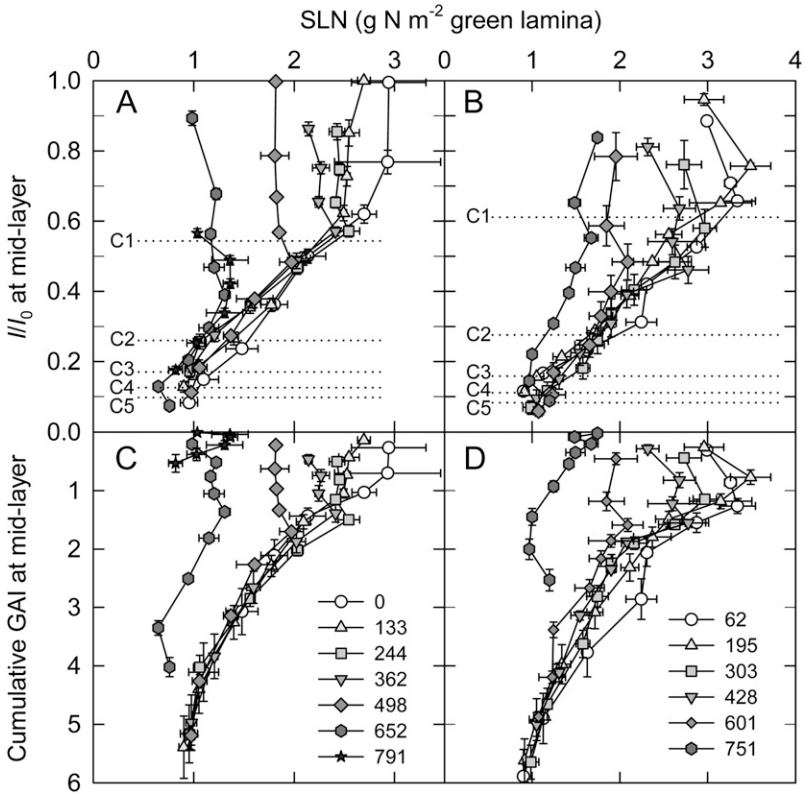

Figure 4. Relative PPFD (A and B) and cumulative GAI counted from the top of the canopy (C and D) versus leaf lamina N mass per unit leaf area at different times (expressed as thermal time; base 0°C) between anthesis and maturity for crops of the bread wheat cultivars Apache (A and C) and Isengrain (B and D) grown in the field with nonlimited N supply. The horizontal dotted lines indicate the height of the collar of the top fertile culm leaves (C1–C5). Data are means ± 1 SE for $n = 3$ independent replicates.

stage, and the small variations observed were most likely due to canopy heterogeneity and differences in sky conditions between the different days of measurements. As a consequence, the presence of brownish, senescent tissues, characterized by different optical properties compared with green tissues, did not affect PPFD distribution. K_L was not significantly different for the two cultivars under study, and the value of 0.42 found here is in good agreement with values previously reported for wheat (Calderini et al., 1997).

The causality of the relationship between PPFD and N vertical distributions has been clearly demonstrated by crop-thinning experiments (Drouet and Bonhomme, 1999) and by inverting the natural gradient of shading (Hikosaka et al., 1994). Changes in the relationship between SLN and PPFD have been related to plant size and N status (Lötscher et al., 2003). There is also some evidence that light quality (in particular the red to far-red ratio) influences N distribution in the canopy (Rousseaux et al., 1999; Frak et al., 2002), but the spectral component of the light gradient is probably less important than the total irradiance component (Pons and de Jong-van Berkel, 2004). It has clearly been demonstrated that accumulation of cytokinins imported through the xylem is involved in the regulation of vertical leaf N distribution (Pons et al., 2001; Boonman et al., 2007). Unexpectedly, in this study, SLN was constant over the length of the flag leaf laminae, although the difference in PPFD between the top and the bottom of the flag leaf laminae was 40%, which was probably associated with similar gradients of transpiration (and thus cytokinin import) and red to far-red ratio. This study does not give information about possible SLN gradient along laminae below the flag leaf, since the canopy layers below the flag leaf collar consisted of lamina segments from different phytomers and tillers. In another experiment, in which SLN was determined at anthesis at three positions along the different laminae of the main culm for two winter bread wheat cultivars grown with low and high N supplies, no significant SLN differences were found along the different laminae (J. Bertheloot and B. Andrieu, unpublished data). Similarly, no difference in SLN has been found along the long and almost erect leaf laminae of tor grass (*Brachypodium pinnatum*; Pons et al., 1993). In maize (*Zea mays*), significant gradients of SLN along individual leaf laminae have been reported during stem elongation but not at silking (Drouet and Bonhomme, 2004) and 55 d later (Hirel et al., 2005). All of these results strongly suggest that, in Poaceae, the PPFD signal is integrated at the whole leaf lamina level and that observed vertical SLN gradients within the canopy are mainly due to differences in SLN between laminae rather than to differences along individual laminae. Thus, the parallel distribution between SLN and I/I_0 observed below the flag leaf collar for horizontal canopy layers is an emerging trait at the canopy level.

At the canopy level, although SLN of the flag leaf laminae started to decrease before any significant

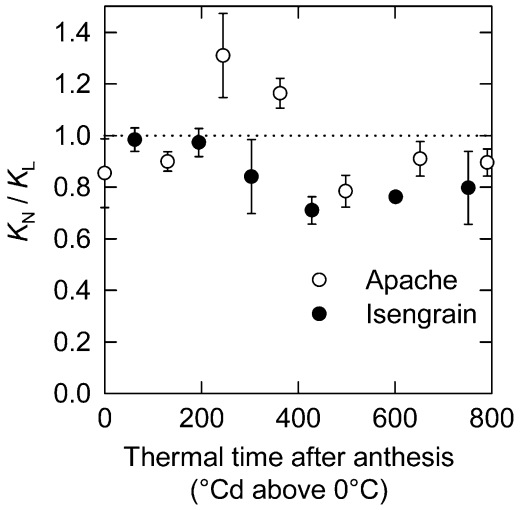

Figure 5. Ratio of N extinction coefficient to light extinction coefficient versus thermal time after anthesis for crops of the bread wheat cultivars Apache and Isengrain grown in the field with nonlimiting N supply. K_N/K_L was calculated by fitting Equation 5, and all regressions were statistically significant (all $P < 0.001$) with r^2 ranging from 0.85 to 0.99. Data are means ± 1 SE for $n = 3$ independent replicates.

reduction of LAI was observed, the relationship between SLN and I/I_0 below the flag leaf collar remained constant until the onset of the phase of rapid GAI decrease. During the phase of rapid GAI decrease, the vertical distribution of SLN changed rapidly and the vertical SLN distribution became more homogeneous. Nevertheless, the vertical N distribution stayed close to optimum between anthesis and approximately 800°Cd later (i.e. until grain filling was almost completed), since K_N/K_L did not change significantly during that period and remained close to 1 (Hirose and Werger, 1987). Similarly, the vertical N distribution in sunflower canopy became more uniform over the course of grain filling and stayed close to the N distribution that optimized canopy photosynthesis almost until crop maturity (Connor et al., 1995). Similar changes in the shape of the vertical SLN profile during the flowering period were reported for natural stands of the tall herb *Solidago altissima* (Schieving et al., 1992). For wheat, vertical SLN gradients close to the optimum have also been reported during the vegetative growth period (Dreccer et al., 2000).

In contrast with results reported for several other species (Drouet and Bonhomme, 2004, and refs. therein), our results showed that for the wheat cultivars under study, both vertical and temporal variations in SLN were mostly due to variations in N concentration. Before 300°Cd after anthesis, the decrease in N concentration in the flag leaf laminae was even more pronounced than that of SLN because of a slight increase in SLM during the first half of the grain-filling period. Decreases in N concentration and SLN in the leaf lamina at the top of the canopy during the first half of grain filling have also been observed in wheat (Bindraban, 1999) and sunflower (Connor et al., 1995).

The Time Course of N Mass per Unit Dry Mass during Grain Filling Is Highly Coordinated among the Different Phytomers

N dynamics during grain filling have mostly been studied for pooled laminae, sheaths, and internodes (Simpson et al., 1983; Ta and Weiland, 1992; Oscarson et al., 1995), but very few studies have analyzed N dynamics for the different vegetative organs during grain filling. Here, we found that total (alive + necrotic

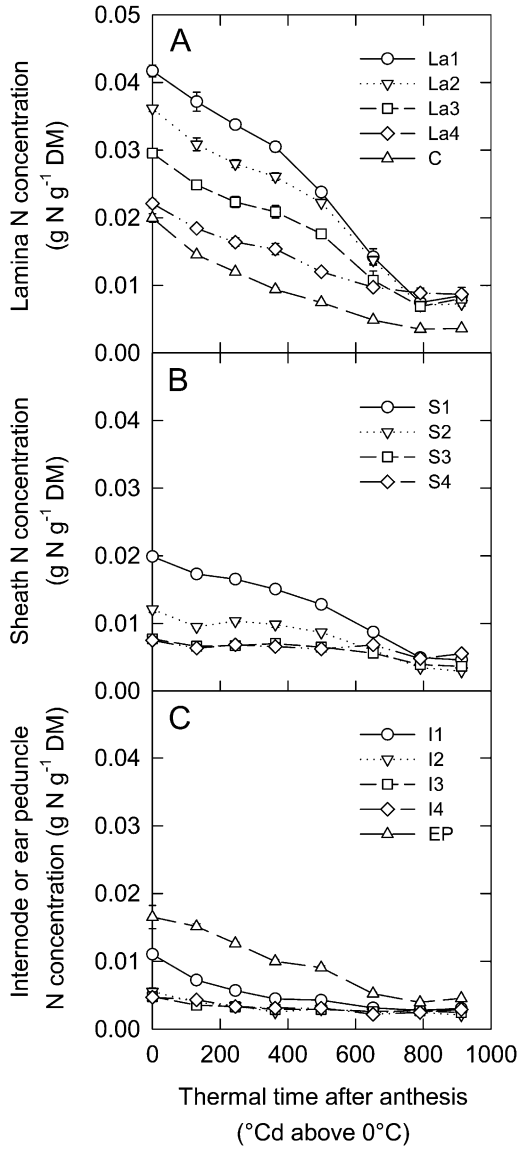

Figure 6. N concentrations for individual leaf laminae (La1–La4) and chaff (denoted C; A), individual leaf sheaths (S1–S4; B), and internodes (I1–I4) and ear peduncles (EP; C) versus thermal time after anthesis for crops of the winter bread wheat cultivar Apache grown in the field with nonlimiting N supply. Data are means ± 1 SE for $n = 3$ independent replicates. DM, Dry mass.

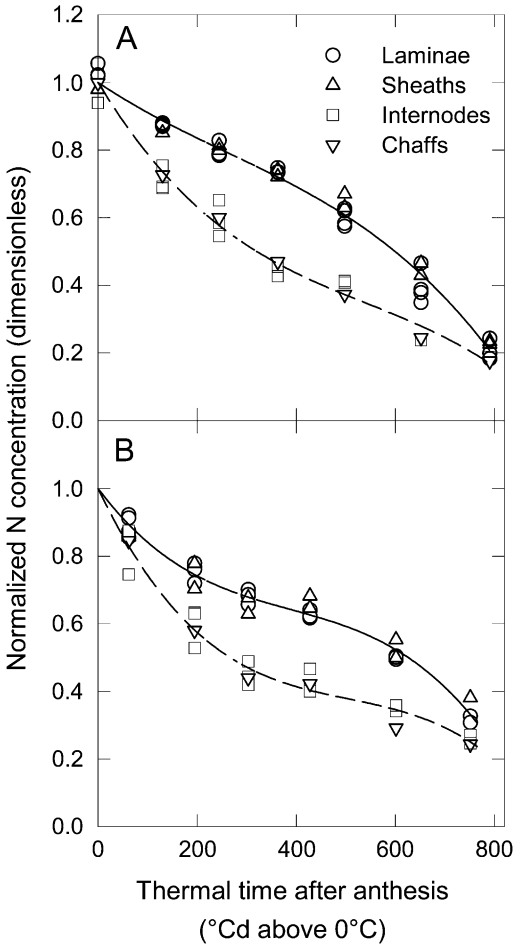

Figure 7. Normalized N concentrations for individual laminae, sheaths, internodes, ear peduncles, and chaff versus thermal time after anthesis for the bread wheat cultivars Apache (A) and Isengrain (B) grown in the field with nonlimiting N supply. Solid lines represent the polynomial functions fitted to normalize lamina and sheath N concentrations; dashed lines represent the polynomial functions fitted to normalize the internode, ear peduncle, and chaff N concentrations. The method used to normalize the N concentrations is described in "Materials and Methods."

tissues) N concentration was positively related to the position along the culm, not only for laminae but also for sheaths and internodes. Within a given phytomer, there was also a systematic ranking between the three organs as a function of their position within the phytomer: N concentration was higher for the lamina than for the sheath and it was higher for the sheath than for the internode. These results are in good agreement with results reported for vegetative wheat crops (Wilhelm et al., 2002). The dependence of N concentration on the organ position along the top fertile culms suggests that vertical N distribution for leaf sheaths and internodes, as for laminae, was related to the PPFD gradient. This assumption is reinforced by the observation that the gradient of N per unit area of sheath tissues between the uppermost and lowermost sheaths was stronger than that observed for lamina tissues (data not shown). The sheaths, because they are vertical organs, mainly intercept PPFD radiation traveling in an almost horizontal direction, whereas laminae, being more horizontal, intercept radiation traveling in a more vertical direction. As a consequence, the PPFD intercepted by the sheaths decreases more rapidly with depth from the top of the canopy than PPFD intercepted by laminae.

During grain filling, despite a stable light gradient, the basipetal gradient of total N concentration decreased for individual sheaths, internodes, and laminae. This reflects a higher rate of N release for the organs richer in N, similar to what has been observed for sunflower (Sadras et al., 1993). Interestingly, the individual leaf laminae and sheaths of the top fertile culms followed very similar patterns of N concentration depletion from anthesis to the end of grain filling, whatever the position along the culm. Similarly, patterns were the same for the individual internodes, the chaff, and the ear peduncle but differed from those of leaves. The fact that N depletion patterns did not depend on organ position shows that N depletion occurs simultaneously in the different vegetative organs of the top fertile culms. The observed concomitant acceleration of N depletion in all organs for Apache in response to the cessation of crop N accumulation supports this view. These results confirm the assumption made by several authors (Thornley, 2004) that soluble proteins in vegetative organs form a unique

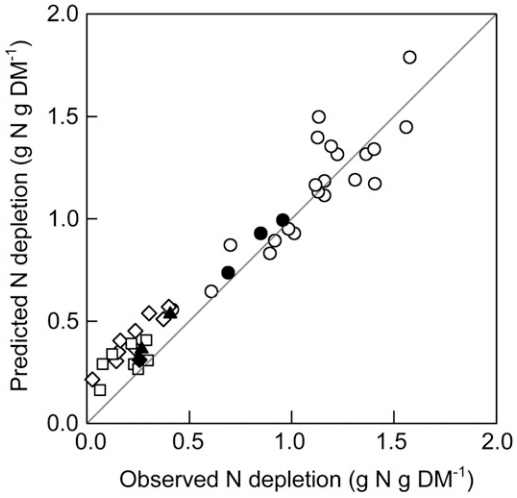

Figure 8. Predicted versus observed N depletion between successive sampling dates after anthesis for individual laminae (circles), sheaths (triangles), and chaff (diamonds) of top fertile culms for the bread wheat cultivar Apache (black symbols) grown in the field with nonlimiting N supply and cultivar Thésée (white symbols) grown in the field with different rates and timings of N supply. For Thésée, leaf sheaths, internodes, and ear peduncles were pooled together (squares). Calculations were restricted to periods of time for which no apparent root N uptake, as estimated from the evolution of whole canopy N mass per unit ground area, was observed. Computation details are given in "Materials and Methods." DM, Dry mass.

pool of N available for growing vegetative and storage organs and that the size of this pool reflects the N status of the plant. The results of Sadras et al. (2000) also head in this direction: they saw no effect of preventing grain development on the vertical patterns of N depletion during the grain-filling period for maize and sunflower and suggested that the effect of sinks on leaf N remobilization and leaf senescence is equally effective throughout the plant.

N Depletion in the Different Vegetative Organs Follows a Unique First-Order Kinetics

In the absence of apparent root N uptake, the N depletion rate of the different organs of the top fertile culms was well described by first-order kinetics for the two growing seasons, two cultivars, and nine N treatments analyzed in this study. This simple model of N depletion is consistent with the proposed model of exponential degradation of Rubisco established from the end of leaf expansion to leaf death (Irving and Robinson, 2006). Exponential degradation of photosynthetic N was also hypothesized in an N distribution model based on the turnover of the photosynthetic apparatus, which assumes that the amount of photosynthetic apparatus of an organ is the result of an equilibrium between its degradation and synthesis (Thornley, 1998, 2004; Kull and Kruijt, 1999). In this model, local light environment plays a major role, since it determines the amounts of photosynthetic N synthesized from metabolic N and carbohydrates synthesized through photosynthesis. Recently, this model has been adapted to analyze N dynamics at the organ level during grain filling of field-grown wheat (Bertheloot et al., 2008).

In the absence of apparent root N uptake, we found a relative rate of N depletion (k) for leaf laminae of 0.0035 $[°Cd]^{-1}$, which is 3.5 times higher than values reported for the degradation of Rubisco for rice (*Oryza sativa*) leaf laminae (Irving and Robinson, 2006). For barley leaves (*Hordeum vulgare*), Peterson et al. (1973) measured rates of Rubisco turnover in the range 0.06 to 0.38 d^{-1}. Considering an average daily temperature of 19.6°C, as observed in both of the experiments reported in this study, the value of k calculated here corresponds to 0.07 d^{-1}, which is in the lower part of the range reported by Peterson et al. (1973). In good agreement with our results, Makino et al. (1984) reported a significant effect of N nutrition on Rubisco content for fully expanded rice leaves, but they did not find any differences in the rate constant of Rubisco degradation during leaf aging. The fact that N depletion in the different leaves follows a first-order kinetics for a wide range of N status is in good agreement with previous results showing that for wheat, grain N accumulation is usually source regulated (Barneix and Guitman, 1993; Martre et al., 2003). Moreover, this result suggests that during grain filling, N translocation from the vegetative organs is limited by the availability of the substrate (proteins) and not by proteolytic processes. To quote Feller and Fischer (1994), ''A fine-tuning of degradative processes inside the plastids may be based on metabolite fluxes across the envelope,'' which may be a mechanism for substrate regulation of protein degradation and N exportation from the vegetative tissues. The genes involved in proteolysis show considerable redundancy (Fischer, 2007), and it has been possible to delay N translocation and leaf senescence through plant transformation (Kato et al., 2004; Robson et al., 2004; Uauy et al., 2006) or mutagenesis (Spano et al., 2003; Donnison et al., 2007) but not to accelerate leaf senescence. Moreover, quantitative trait loci identified for leaf protease activities indicated no functional role for the enzymes involved in plant N recycling or the control of grain protein concentration (Yang et al., 2004). During grain filling of wheat, changes in aminopeptidase and carboxypeptidase activity have been shown to parallel changes in protein concentration of vegetative organs (Feller et al., 1977; Waters et al., 1980). Finally, the expression of the cytosolic Gln synthetase, which is involved in the conversion of Glu to Gln, the major form of N transport in the phloem sap of most cereals, is positively regulated by several amino acids, including Glu (Masclaux-Daubresse et al., 2005). Taken together with our results, these studies demonstrate that the remobilization of vegetative N during grain filling is regulated by the N concentration of the vegetative tissues rather than by proteolytic or transport processes. Even so, higher rates of N remobilization were associated with the higher grain protein concentration of nearly isogenic recombinant substitution lines carrying the high grain protein concentration *Gpc-B1* locus from wild emmer wheat (*Triticum turgidum* subsp. *dicoccoides*; Kade et al., 2005; Uauy et al., 2006). All of these results indicate that efforts to increase N availability during grain filling should focus on processes related to N assimilation and temporary storage in vegetative organs rather than on protein degradation and translocation. However, it would be worth analyzing the genetic variability of the rate constant of Rubisco degradation. Investigations should be undertaken to determine if cultivars with low rate constants of Rubisco degradation and a subsequent longer leaf life span can be selected.

CONCLUSION

In summary, this study clearly illustrates that N dynamics in the canopy is integrated at the plant level and strongly depends on the local PPFD conditions defined by the structure of the canopy. Despite the fact that the green area of the top fertile culm leaves decreased sequentially from the bottom to the top of the canopy and that laminae La3 and La4 were fully yellow before any significant decrease of the green area of La1 could be observed, leaf N depletion appeared to be well synchronized across the phytomers, implying that the remobilization of N is regulated at

the plant level and not at the organ level. Moreover, our results strongly suggest that the turnover of proteins in vegetative organs is regulated by the amount of substrate (proteins) available. Is the vertical leaf N distribution related to light distribution during the grain-filling period? This is the case below the flag leaf, where the vertical lamina N distribution paralleled the PPFD gradient almost until the end of grain filling; however, the significant PPFD gradient along the flag leaf lamina was not associated with a SLN gradient. During grain filling, SLN started to decrease from the top of the canopy, which tended to flatten the vertical SLN gradient. Does the time course of N concentration during grain filling follow a similar pattern in all vegetative organs? This is partially verified, since the time course of N concentration of the different laminae and sheaths of the top fertile culms, on the one hand, and of the internodes and chaff, on the other hand, followed similar patterns. More specifically, does N depletion in the different vegetative organs follow unique first-order kinetics in the period of no apparent root N uptake? This appeared to be partially the case, since N depletion of all vegetative organs followed first-order kinetics, but the rate constant of N depletion was higher for leaf laminae than for the stems, leaf sheaths, and chaff. This analysis of the spatiotemporal distribution of N during grain filling makes it possible to define simple rules to model the distribution of N during grain filling, which should lead to the development of a mechanistic simulation model of N dynamics for cereals (Bertheloot et al., 2008). Coupled with a mechanistic model of leaf photosynthesis, such a model would allow scaling up the rules described here to the whole crop level to analyze their consequences for crop productivity and N use efficiency and grain yield and to analyze strategies to improve grain yield and N use efficiency.

MATERIALS AND METHODS

Plant Material and Growing Conditions

All experiments were carried out in the field at Clermont-Ferrand, France (45°47′ N, 3°10′ E, 329 m elevation). In the first experiment (experiment 1), the vertical distribution of light and N were studied during the reproductive stage both per organ (individual leaf laminae, leaf sheaths, and internodes, chaff, and grains) and per vertical canopy layer for the winter bread wheat (*Triticum aestivum*) cultivars Apache and Isengrain, the two most grown cultivars in France. Both cultivars were sown on November 14, 2004, at a density of 280 seeds m^{-2} as part of a larger experiment including 120 doubled haploid lines. The experimental design was a randomized complete block design with three replicates. Plots were 5.0 m long and eight rows wide, with a row spacing of 0.16 m (7.2 m^2). Anthesis was recorded on May 27 and 28, 2005, for Apache and Isengrain, respectively. Crops were rain fed and received 295 and 64 mm of rainfall from sowing to anthesis and from anthesis to physiological maturity, respectively. No symptom of water deficit was observed during the grain-filling period. Average air temperature from sowing to anthesis and from anthesis to grain maturity was 7°C and 19.6°C, respectively. Mineral soil N at the end of winter (February 17, 2005) was 12.3 g N m^{-2} in the 0.9-m-deep soil profile. Forty seven percent and 37% of the mineral soil N were in the 0- to 30-cm and 30- to 60-cm soil layers, respectively. The crops received 4, 4, 6, and 10 g N m^{-2} ammonium nitrate at one node, meiosis, heading, and anthesis, respectively. Pests and diseases were controlled chemically.

In the second experiment in 1994 (experiment 2), the effect of preanthesis and postanthesis N availability in the soil on N translocation during grain filling was studied in the field for the bread wheat cultivar Thésée. This experiment has been described in detail elsewhere (Martre et al., 2003; Triboi et al., 2003). In brief, three preanthesis N treatments, low (L), medium (M), and high (H), were factorized with three postanthesis N treatments, 0 (H0, L0, M0), 1 (L1, H1, M1), and 2 (L2, M2, H2). At anthesis, whole canopy N per unit ground area ranged from 2.30 ± 0.01 g N m^{-2} for the L treatments to 6.37 ± 0.22 g N m^{-2} for the H treatments. Whole canopy postanthesis N accumulation ranged from 1.58 ± 0.35 g N m^{-2} for the 0 treatments to 7.83 ± 0.33 g N m^{-2} for L2 and M2 and to 6.34 ± 0.30 g N m^{-2} for H2.

Daily weather data were recorded at a weather station adjacent to the field plots. Thermal time was calculated by summing daily degree-days (°Cd) above 0°C, which were calculated as the average between maximum and minimum daily air temperatures.

Plant Sampling

In experiment 1, the time courses of dry mass and N mass were monitored for both cultivars by weekly destructive sampling from anthesis to crop maturity. Two independent sampling protocols were used. In the first, plants were dissected according to their botanical structure with phytomer numbered basipetally. In each phytomer, lamina, sheath, and internode were separated. In the second protocol, the canopy was clipped into horizontal layers. This allowed analyzing N contents of leaf laminae and stems (leaf sheaths, internodes, and ear peduncle pooled together) according to their vertical position and light environment. The two types of samplings were carried out on adjacent rows. For laminae, alive (identified by their greenish color) and dead/nonphotosynthetic (identified by their brownish color) tissues were analyzed separately.

For the sampling per phytomer, three rows × 0.5-m long were sampled. The fresh mass of the samples was determined and the plants were counted. Fifteen plants, with fresh mass within 5% of the average fresh mass per plant, were subsampled and analyzed. The culms of the 15 plants were separated from each other, and the top fertile culms (i.e. the main stem and the first two tillers) were dissected into their individual organs.

For the stratified-clipping method, a 0.28-m^2 metallic frame (0.44 × 0.64 m) was positioned above the canopy, leaving two border rows on each side. The canopy within the frame was cut from the base of the ears of the top fertile culms to the ground level into 5- to 12-cm-thick layers, resulting in nine to 10 layers. Layer thicknesses were determined so that each layer intercepted 10% to 15% of the light intercepted by the whole canopy. In the laboratory, the cut plant material from each layer was divided into chaff, grains, stems (including leaf sheaths), and alive and dead/nonphotosynthetic lamina tissues. All of the collected material was analyzed.

In experiment 2, 0.2-m^2 samples were taken in each plot at anthesis and 290°Cd, 505°Cd, 712°Cd, and 900°Cd later. Plants were subsampled as for the sampling per phytomer in experiment 1. Individual leaf laminae, whole stems (all internodes, leaf sheaths, and ear peduncles pooled together), and ear chaff were separated from each other and analyzed. Three replicates were used per N treatment.

Canopy and Plant Structure

Canopy structure was evaluated by the GAI (surface area of green tissues per unit ground area) and LAI (surface area of green lamina per unit ground area) for each canopy horizontal layer. The projected surface areas of the green parts of laminae, stems, and ears were determined using a Li-3100 Area Meter (Li-Cor). To calculate GAI, the projected surface areas of stems, internodes, and ears were multiplied by $\pi/2$ (Lang, 1991). The heights from the soil of the individual leaf collars were estimated from the measured lengths of leaf sheaths and internodes.

Dry Mass, N Concentration Determinations, and SLN and SLM Calculations

Dry mass was determined after oven drying at 80°C until constant mass. The samples were then ground, and their N mass per unit dry mass (N concentration) was determined. In experiment 1, total N concentration was determined by elemental analysis using a Carlo Erba 1110 analyzer. In experiment 2, total N concentration was determined by the micro-Kjeldahl

method using a Kjeltec 2300 analyzer (Foss Tecator). SLN (g N m^{-2} leaf lamina) and SLM (g dry mass m^{-2} [laminae]) were calculated by dividing the N concentration and dry mass of alive leaf lamina tissues, respectively, by their green surface area. Mean canopy SLN and SLM were calculated by dividing the mass of total living leaf lamina N per unit ground area and dry mass by LAI, respectively.

Light Measurements

The vertical distribution of PPFD (μmol m^{-2} s^{-1}) was determined 1 d before plant sampling using a 90-cm-long linear ceptometer (LP-80 AccuPAR; Decagon Devices) equipped with an external PPFD sensor. Simultaneous measurements above and within the canopy were taken in the area of the next plant sampling. The ceptometer was inserted in the canopy at 45° from the rows, and measurements were taken every 5 to 10 cm from the top of the canopy to the ground level. Vertical profiles of PPFD were determined in triplicate for each plot. All measurements were done between 11:00 AM and 13:00 PM.

Calculation of Light and N Extinction Coefficients

PPFD was assumed to be attenuated through the canopy following the Lambert-Beer's law (Monsi and Saeki, 2005):

$$I = I_0 \exp(-K_L \times F) \quad (1)$$

where F (m^2 green tissue m^{-2} ground) is the cumulative GAI from the top of the canopy; K_L (m^2 ground m^{-2} green tissue) is the light extinction coefficient; and I_0 and I (μmol m^{-2} s^{-1}) are the PPFD on a horizontal level above the canopy and at depth F, respectively. K_L was estimated after logarithmic transformation of Equation 1. SLN was related to I/I_0 by:

$$SLN = (SLN_0 - n_b)\exp(-K_N \times F) + n_b \quad (2)$$

where SLN_0 and SLN are SLN at the top of the canopy and at depth F, respectively; K_N is the N extinction coefficient (m^2 ground m^{-2} green tissue); and n_b (g N m^{-2} leaf lamina) is SLN at which light-saturated photosynthesis is null. The vertical gradient of SLN was described as a function of the absolute cumulative leaf area index and not the relative one, as has often been done (Hirose and Werger, 1987), because the leaf area index varies considerably during the grain-filling period. By eliminating F from Equations 1 and 2, the relationship between SLN and the relative PPFD (I/I_0) can be rewritten as:

$$SLN = (SLN_0 - n_b)\left(\frac{I(z)}{I_0}\right)^{(K_N/K_L)} + n_b \quad (3)$$

An optimal SLN distribution is given when K_L equals K_N (Anten et al., 1995) and thus K_N/K_L equals 1. For wheat, the average of the values reported for n_b is 0.4 g N m^{-2} (Araus and Tapia, 1987; Bindraban, 1999; Dreccer et al., 2000). K_L/K_N was estimated after logarithmic transformation of Equation 3 with n_b set at 0.4 g N m^{-2}.

Rescaling of the N Concentration Patterns for Individual Organs during the Reproductive Stage

In order to test the hypothesis that time courses of N concentrations for individual organs of top fertile culms differed only by a scaling factor, the scaling coefficient S_{ls} was first calculated for the lamina and sheath of each phytomer. S_{ls} was calculated as the slope of the regression between N concentration measured at different dates for a given lamina or sheath and for the uppermost lamina, denoted La1. Then the normalized N concentration $N_{ls}(t)/S_{ls}$ was calculated for each lamina and sheath and a unique polynomial function of thermal time, $F_{ls}(t)$, was fitted to the data set formed by the normalized N concentrations:

$$F_{ls}(t) = (1 + \alpha_{ls}(t) + \beta_{ls}(t^2) + \delta_{ls}(t^3)) \quad (4)$$

where α_{ls}, β_{ls}, and δ_{ls} are empirical coefficients and t (°Cd above 0°C) is the thermal time after anthesis. $F_{ls}(t)$ represents the shared pattern of N dynamics in laminae and sheaths from anthesis to the end of grain filling.

The same analysis was performed for internodes, chaff, and the ear peduncle, using the uppermost internode I1 to normalize their patterns.

Modeling of N Depletion Kinetics

In the period of no apparent root N uptake, N depletion in individual organs was modeled using a negative exponential function:

$$N(t) = N_0 \exp(-kt) \quad (5)$$

where t (°Cd above 0°C) is thermal time after anthesis, N (g N g^{-1}) is N concentration on a dry mass basis, N_0 represents N concentration estimated at anthesis, and k ($[°Cd]^{-1}$) is the relative rate of N depletion. k and N_0 were determined after logarithmic transformation of Equation 5. A fitted value of N_0 was determined for each organ of each phytomer and treatment, whereas a unique fitted value of k was determined for every lamina and treatment.

In order to evaluate the above model, we used the value of k determined for the laminae of Thésée to predict the quantity of N depleted between successive sampling dates:

$$\Delta N_{t_1 t_2} = N(t_1)(\exp(-k(\Delta t)) - 1) \quad (6)$$

where Δt is the thermal time between two successive sampling dates.

Statistics

Statistical analyses were done using Statgraphics Plus 4.1 for Windows (Statistical Graphics) or R for Windows (http://www.r-project.org). Differences between cultivars in GAI, LAI, SLN, and SLM as well as N content and concentration at anthesis were analyzed using unpaired t tests after checking that data followed a normal distribution. For a given cultivar, differences in K_L and K_N/K_L during grain filling were analyzed using one-way ANOVA (α = 0.05) after checking that data followed a normal distribution and that variances were not statistically different. To determine the rate and duration of accumulation of grain N and dry mass, data were fitted with a three-parameter logistic function (Triboi et al., 2003). The first-order kinetics model of N depletion in vegetative organs was evaluated using Equation 6. Goodness of fit of the model was evaluated using the RMSE (Kobayashi and Salam, 2000) and the RRMSE. The RRMSE was determined by dividing the RMSE by the mean of the observed values and then multiplying by 100.

ACKNOWLEDGMENTS

We thank J. Messaoud, B. Bonnemoy, J.-L. Joseph, and P. Lemaire for their skillful technical assistance, and V. Allard, J. Le Gouis, and D. Moreau (INRA Clermont-Ferrand) and B. Hirel (INRA Versailles) for helpful comments on the manuscript.

Received June 5, 2008; accepted September 11, 2008; published September 17, 2008.

LITERATURE CITED

Anten NPR, Hirose T, Onoda Y, Kinugasa T, Kim HY, Okada MKK (2004) Elevated CO_2 and nitrogen availability have interactive effects on canopy carbon gain in rice. New Phytol **161:** 459–471

Anten NPR, Schieving F, Werger MJA (1995) Patterns of light and nitrogen distribution in relation to whole canopy carbon gain in C_3 and C_4 mono and dicotyledonous species. Oecologia **101:** 504–513

Araus JL, Tapia L (1987) Photosynthetic gas exchange characteristics of wheat flag leaf blades and sheaths during grain filling: the case of a spring crop grown under Mediterranean climate conditions. Plant Physiol **85:** 667–673

Austin RB (1999) Yield of wheat in the United Kingdom: recent advances and prospects. Crop Sci **39:** 1604–1610

Barneix AJ, Guitman MR (1993) Leaf regulation of the nitrogen concentration in the grain of wheat plants. J Exp Bot **44:** 1607–1612

Bertheloot J, Andrieu B, Fournier C, Martre P (2008) A process-based model to simulate nitrogen distribution within wheat (*Triticum aestivum* L.) during grain filling. Funct Plant Biol (in press)

Bindraban PS (1999) Impact of canopy nitrogen profile in wheat on growth. Field Crops Res **63:** 63–77

Boonman A, Prinsen E, Gilmer F, Schurr U, Peeters AJM, Voesenek LACJ,

Pons TL (2007) Cytokinin import rate as a signal for photosynthetic acclimation to canopy light gradients. Plant Physiol **143:** 1841–1852

Borrell A, Hammer G, van Oosterom E (2001) Stay-green: a consequence of the balance between supply and demand for nitrogen during grain filling? Ann Appl Biol **138:** 91–95

Calderini DF, Dreccer MF, Slafer GA (1997) Consequences of breeding on biomass, radiation interception and radiation-use efficiency in wheat. Field Crops Res **52:** 271–281

Chen JL, Reynolds JF, Harley PC, Tenhunen JD (1993) Coordination theory of leaf nitrogen distribution in a canopy. Oecologia **93:** 63–69

Connor DJ, Sadras VO, Hall AJ (1995) Canopy nitrogen distribution and the photosynthetic performance of sunflower crops during grain filling: a quantitative analysis. Oecologia **101:** 274–281

Donnison IS, Gay AP, Thomas H, Edwards KJ, Edwards D, James CL, Thomas AM, Ougham HJ (2007) Modification of nitrogen remobilization, grain fill and leaf senescence in maize (Zea mays) by transposon insertional mutagenesis in a protease gene. New Phytol **173:** 481–494

Dreccer MF, Slafer GA, Rabbinge R (1998) Optimization of vertical distribution of canopy nitrogen: an alternative trait to increase yield potential in winter cereals. J Crop Prod **1:** 47–77

Dreccer MF, Van Oijen M, Schapendonk AHCM, Pot CS, Rabbinge R (2000) Dynamics of vertical leaf nitrogen distribution in a vegetative wheat canopy: impact on canopy photosynthesis. Ann Bot (Lond) **86:** 821–831

Drouet JL, Bonhomme R (1999) Do variations in local leaf irradiance explain changes to leaf nitrogen within row maize canopies? Ann Bot (Lond) **84:** 61–69

Drouet JL, Bonhomme R (2004) Effect of 3D nitrogen, dry mass per area and local irradiance on canopy photosynthesis within leaves of contrasted heterogeneous maize crops. Ann Bot (Lond) **93:** 699–710

Evans JR (1989) Partitioning of nitrogen between and within leaves grown under different irradiances. Aust J Plant Physiol **16:** 533–548

Feller U, Fischer A (1994) Nitrogen metabolism in senescing leaves. Crit Rev Plant Sci **13:** 241–273

Feller UK, Soong TST, Hageman RH (1977) Leaf proteolytic activities and senescence during grain development of field-grown corn (*Zea mays* L.). Plant Physiol **59:** 290–294

Field C (1983) Allocating leaf nitrogen for the maximization of carbon gain: leaf age as a control on the allocation program. Oecologia **56:** 341–347

Fischer A (2007) Nutrient remobilization during leaf senescence. *In* S Gan, ed, Annual Plant Reviews, Vol 26. Blackwell Publishing, Oxford, pp 87–107

Frak E, Le Roux X, Millard P, Adam B, Dreyer E, Escuit C, Sinoquet H, Vandame M, Varlet-Grancher C (2002) Spatial distribution of leaf nitrogen and photosynthetic capacity within the foliage of individual trees: disentangling the effects of local light quality, leaf irradiance, and transpiration. J Exp Bot **53:** 2207–2216

Hikosaka K, Terashima I, Katoh S (1994) Effects of leaf age, nitrogen nutrition and photon flux density on the distribution of nitrogen among leaves of a vine (*Ipomoea tricolor* Cav.) grown horizontally to avoid mutual shading of leaves. Oecologia **97:** 451–457

Hirel B, Andrieu B, Valadier MH, Renard S, Quillere I, Chelle M, Pommel B, Fournier C, Drouet JL (2005) Physiology of maize. II. Identification of physiological markers representative of the nitrogen status of maize (Zea mays) leaves during grain filling. Physiol Plant **124:** 178–188

Hirose T, Werger MJA (1987) Maximizing daily canopy photosynthesis with respect to the leaf nitrogen allocation pattern in the canopy. Oecologia **72:** 520–526

Irving LJ, Robinson D (2006) A dynamic model of Rubisco turnover in cereal leaves. New Phytol **169:** 493–504

Kade M, Barneix AJ, Olmos S, Dubcovsky J (2005) Nitrogen uptake and remobilization in tetraploid 'Langdon' durum wheat and a recombinant substitution line with the high grain protein gene Gpc-B1. Plant Breed **124:** 343–349

Kato Y, Murakami S, Yamamoto Y, Chatani H, Kondo Y, Nakano T, Yokota A, Sato F (2004) The DNA-binding protease, CND41, and the degradation of ribulose-1,5-bisphosphate carboxylase/oxygenase in senescent leaves of tobacco. Planta **97:** 97–104

Kim HY, Lieffering M, Miura S, Kobayashi K, Okada M (2001) Growth and nitrogen uptake of CO_2-enriched rice under field conditions. New Phytol **150:** 223–229

Kobayashi K, Salam MU (2000) Comparing simulated and measured values using mean squared deviation and its components. Agron J **92:** 345–352

Kull O (2002) Acclimation of photosynthesis in canopies: models and limitations. Oecologia **133:** 267–279

Kull O, Kruijt B (1999) Acclimation of photosynthesis to light: a mechanistic approach. Funct Ecol **13:** 24–36

Lang ARG (1991) Application of some of Cauchy's theorems to estimation of surface areas of leaves, needles and branches of plants, and light transmittance. Agric For Meteorol **55:** 191–212

Lötscher M, Stroh K, Schnyder H (2003) Vertical leaf nitrogen distribution in relation to nitrogen status in grassland plants. Ann Bot (Lond) **92:** 679–688

Makino A, Mae T, Ohiro K (1984) Relation between nitrogen and ribulose-1,5-bisphosphate carboxylase in rice leaves from emergence through senescence. Plant Cell Physiol **25:** 429–437

Martre P, Porter JR, Jamieson PD, Triboï E (2003) Modeling grain nitrogen accumulation and protein composition to understand the sink/source regulations of nitrogen remobilization for wheat. Plant Physiol **133:** 1959–1967

Martre P, Semenov MA, Jamieson PD (2007) Simulation analysis of physiological traits to improve yield, nitrogen use efficiency and grain protein concentration in wheat. *In* JHJ Spiertz, PC Struik, HH Van Laar, eds, Scale and Complexity in Plant Systems Research, Gene-Plant-Crop Relations. Springer, Dordrecht, The Netherlands, pp 181–201

Masclaux-Daubresse C, Carrayol E, Valadier M-H (2005) The two nitrogen mobilisation- and senescence-associated *GS1* and *GDH* genes are controlled by C and N metabolites. Planta **221:** 580–588

Monsi M, Saeki T (2005) On the factor light in plant communities and its importance for matter production. Ann Bot (Lond) **95:** 549–567

Mooney HA, Gulmon SL (1979) Environmental and evolutionary constraints on the photosynthetic characteristics of higher plants. *In* OT Solbrig, S Jain, GB Johnson, PH Raven, eds, Topics in Plant Population Biology. Columbia University Press, New York, pp 316–337

Oscarson P, Lundborg T, Larsson M, Larsson CM (1995) Genotypic differences in nitrate uptake and nitrogen utilization for spring wheat grown hydroponically. Crop Sci **35:** 1056–1062

Peterson LW, Kleinkopf GE, Huffaker RC (1973) Evidence for lack of turnover of ribulose 1,5-diphosphate carboxylase in barley leaves. Plant Physiol **51:** 1042–1045

Pons TL, de Jong-van Berkel YEM (2004) Species-specific variation in the importance of the spectral quality gradient in canopies as a signal for photosynthetic resource partitioning. Ann Bot (Lond) **94:** 725–732

Pons TL, Jordi W, Kuiper D (2001) Acclimation of plants to light gradients in leaf canopies: evidence for a possible role for cytokinins transported in the transpiration stream. J Exp Bot **52:** 1563–1574

Pons TL, Van Rijnbeck H, Scheurwater I, Van Der Verf A (1993) Importance of the gradient in photosynthetically active radiation in a vegetation stand for leaf nitrogen allocation in two monocotyledons. Oecologia **95:** 416–424

Reynolds JF, Chen J (1996) Modelling whole-plant allocation in relation to carbon and nitrogen supply: coordination versus optimization. Opinion. Plant Soil **185:** 65–74

Robson PRH, Donnison IS, Wang K, Frame B, Pegg SE, Thomas A, Thomas H (2004) Leaf senescence is delayed in maize expressing the *Agrobacterium IPT* gene under the control of a novel maize senescence-enhanced promoter. Plant Biotechnol J **2:** 101–112

Rousseaux MC, Hall AJ, Sanchez RA (1999) Light environment, nitrogen content, and carbon balance of basal leaves of sunflower canopies. Crop Sci **39:** 1093–1100

Sadras VO, Echarte L, Andrade FH (2000) Profiles of leaf senescence during reproductive growth of sunflower and maize. Ann Bot (Lond) **85:** 187–195

Sadras VO, Hall AJ, Connor DJ (1993) Light-associated nitrogen distribution profile in flowering canopies of sunflower (*Helianthus annuus* L.) altered during grain growth. Oecologia **95:** 488–494

Schieving F, Werger MJA, Hirose T (1992) Canopy structure, nitrogen distribution and whole canopy photosynthetic carbon gain in growing and flowering stands of tall herbs. Vegetatio **102:** 173–181

Shearman VJ, Sylvester-Bradley R, Scott RK, Foulkes MJ (2005) Physiological processes associated with wheat yield progress in the UK. Crop Sci **45:** 175–185

Simpson RJ, Lambers H, Dalling MJ (1983) Nitrogen redistribution during grain growth in wheat. IV. Development of a quantitative model of the translocation of nitrogen to the grain. Plant Physiol **71:** 7–14

Spano G, Di Fonzo N, Perrotta C, Platani C, Ronga G, Lawlor DW, Napier JA, Shewry PR (2003) Physiological characterization of 'stay green' mutants in durum wheat. J Exp Bot **54:** 1415–1420

Ta CT, Weiland RT (1992) Nitrogen partitioning in maize during ear development. Crop Sci **32:** 443–451

Thornley JHM (1998) Dynamic model of leaf photosynthesis with acclimation to light and nitrogen. Ann Bot (Lond) **81:** 421–430

Thornley JHM (2004) Acclimation of photosynthesis to light and canopy nitrogen distribution: an interpretation. Ann Bot (Lond) **93:** 473–475

Triboi E, Martre P, Triboi-Blondel AM (2003) Environmentally-induced changes of protein composition for developing grains of wheat are related to changes in total protein content. J Exp Bot **54:** 1731–1742

Triboi E, Triboi-Blondel AM (2002) Productivity and grain or seed composition: a new approach to an old problem. Invited Paper. Eur J Agron **16:** 163–186

Uauy C, Brevis JC, Dubcovsky J (2006) The high grain protein content gene Gpc-B1 accelerates senescence and has pleiotropic effects on protein content in wheat. J Exp Bot **57:** 2785–2794

Waters SP, Peoples MB, Simpson RJ, Dalling MJ (1980) Nitrogen redistribution during grain growth in wheat (*Triticum aestivum* L.). 1. Peptide hydrolase activity and protein breakdown in the flag leaf, glumes and stem. Planta **148:** 422–428

Wilhelm WW, McMaster GS, Harrell DM (2002) Nitrogen and dry matter distribution by culm and leaf position at two stages of vegetative growth in winter wheat. Agron J **94:** 1078–1086

Yang L, Mickelson S, See D, Blake TK, Fischer AM (2004) Genetic analysis of the function of major leaf proteases in barley (*Hordeum vulgare* L.) nitrogen remobilization. J Exp Bot **55:** 2607–2616